Mechanism of the ultraviolet photodissociation of chloroethylenes determined from the Doppler profiles, spatial anisotropy, and power dependence of the photofragments

ARTICLE *in* THE JOURNAL OF CHEMICAL PHYSICS · OCTOBER 1992

Impact Factor: 2.95 · DOI: 10.1063/1.463836

Mechanism of the ultraviolet photodissociation of chloroethylenes determined from the Doppler profiles, spatial anisotropy, and power dependence of the photofragments

Yuxiang Mo,[a] Kenichi Tonokura, Yutaka Matsumi, and Masahiro Kawasaki
Institute for Electronics Science, Hokkaido University, Sapporo 060, Japan

Tetsuya Sato and Tatsuo Arikawa
Department of Applied Physics, Tokyo University of Agriculture and Technology, Koganei 184, Japan

Peter T. A. Reilly, Yongjin Xie,[b] Yung-an Yang, Yibo Huang, and Robert J. Gordon
Department of Chemistry (m/c 111), University of Illinois at Chicago, Box 4348, Chicago Illinois 60680

(Received 20 March 1992; accepted 3 June 1992)

Doppler profiles of chlorine and hydrogen atomic fragments produced in the photodissociation of mono- and dichloroethylenes at 193 nm have been measured in a pump-and-probe experiment using 2+1 resonance-enhanced multiphoton ionization. In a second experiment, the angular distributions of the Cl fragments produced from chloroethylenes at 235 and 238 nm were measured using a perfect-focusing mass spectrometer. In a third experiment, we measured the power dependence of the relative yields of H, Cl, HCl, and HCl^+ produced from vinyl chloride at 193 nm. For Cl detachment, two primary processes have been confirmed. One produces an isotropic angular distribution of photofragments, while the other produces an anisotropic distribution. For H atom detachment, an isotropic angular distribution and a Boltzmann velocity distribution were found. The ratio of yields of the Cl and H fragments was found to be 4 ± 1 for CH_2CCl_2 and higher than 10 for *t*-CHClCHCl and CCl_2CClH. The H, Cl, and HCl yields were found to be first order in laser intensity, while the HCl^+ yield was found to be third order. Saturation measurements of the ion yield indicate that the latter results from a 1+1+1 resonance-enhanced process involving a bound state of the parent molecule. This intermediate state may also be responsible for producing the statistical component of the Cl atom product.

I. INTRODUCTION

Chloroethylenes have strong absorption bands around 200 nm which are assigned to the (π,π^*) transition. Although the photochemistry of chloroethylenes in this region has been studied extensively,[1-13] the details of the reaction mechanism are still poorly understood. One reason for this is that in this energy region there are a variety of possible electronic transitions from the C=C π orbital and the chlorine n orbitals to the π^*, σ^*, and 3s Rydberg orbitals which may all participate in the dissociation of the excited molecule. In this paper, we present experimental evidence for several competing mechanisms.

For one-photon photodissociation of vinyl chloride at 193 nm, the following pathways are energetically[14-18] allowed:

$$CH_2CHCl+193\ \text{nm}\rightarrow HCCH(X\,^1\Sigma_g^+)+H(^2S)+Cl(^2P_j),\qquad E_{avl}=21.2\pm0.4\ \text{kcal/mol},\qquad (1)$$

$$CH_2CHCl+193\ \text{nm}\rightarrow CH_2CCl(X)+H(^2S),\qquad E_{avl}=48,\qquad (2)$$

$$CH_2CHCl+193\ \text{nm}\rightarrow CH_2CH(X,\ \tilde{A})+Cl(^2P_j),\qquad E_{avl}=59\pm2,\ 15\pm2,\qquad (3)$$

$$CH_2CHCl+193\ \text{nm}\rightarrow HCCH(X\,^1\Sigma_g^+)+HCl(X\,^1\Sigma^+),\qquad E_{avl}=124.2\pm0.4,\qquad (4a)$$

$$CH_2CHCl+193\ \text{nm}\rightarrow H_2CC(^1A_1,\ ^3B_2)+HCl(X\,^1\Sigma^+),\qquad E_{avl}=81\pm2,\ 39\pm4.\qquad (4b)$$

Reactions (4a) and (4b) denote, respectively, four-center and three-center elimination of HCl. Reactions (3) and (4b) include the possibilities of producing electronically excited vinyl and vinylidene radicals.

Umemoto *et al.*[1] have reported the translational energy distributions of reactions (3) and (4) obtained from a time-of-flight experiment. They found that there are two pathways to produce Cl fragments from dichloroethylenes at 193 nm. One yields fragments with a high translational energy (peaked at approximately 20 kcal/mol) which result from crossing of the photoprepared (π,π^*) state to the repulsive (n,σ^*) state. The other produces low energy fragments ($\sim$6 kcal/mol) resulting from the internal conversion process $(\pi,\pi^*)\rightarrow(\pi,\sigma^*)\rightarrow(n,\sigma^*)$. They also re-

[a] On leave from the Laboratory for Molecular Reaction Dynamics, Dalian Institute of Chemical Physics, Dalian 116011, China.
[b] Permanent address: Excel Technology, Inc., 101-2 Colin Dr., Holbrook, NY 11741.

 0021-9606/92/194815-12$006.00

ported the branching ratio of reactions (3) and (4) and the anisotropy parameters of the photofragments for these two pathways. Vibrational energy distributions of HCl fragments ($v \geqslant 1$) have been determined for CH_2CHCl and *t*-CHClCHCl by time-resolved Fourier transform infrared (FTIR) measurement of the photofragment emission spectrum.[3] Rotational state distributions of HCl($v=0$, 1, and 2) from vinyl chloride at 193 nm have been determined by resonance enhanced multiphoton ionization (REMPI) detection in a pump-and-probe experiment.[9]

In the present paper, we report Doppler profiles of Cl and H at 193 nm and the spatial anisotropy of the Cl fragment at 235 and 238 nm for several chloroethylenes. We also report the power dependence of the nascent H, Cl, HCl, and HCl^+ produced from vinyl chloride at 193 nm.

The HCl^+ product requires absorption of at least three 193 nm photons. A previous report[4] of this product attributed it to a two-photon ionization of nascent HCl. We provide evidence for a different mechanism which is more closely linked to the atomic detachment processes.

While there have been numerous studies of Cl and HCl formation from these molecules, this is the first report of H atom detachment. We propose here a modified statistical model which accounts for the kinetic energy of the recoiling H fragment.

II. EXPERIMENT

A. Doppler spectroscopy

The experimental setup for MPI Doppler spectroscopy of the photofragments was described in detail in a previous report.[19] Briefly, the molecular beam, the dissociation laser, and the probe laser beams are intersected mutually perpendicularly. The 193 nm photolysis beam (10 Hz, approximately 10 mJ/cm^2) passed through a 5 mm iris and was polarized by a pile-of-plates polarizer, which consisted of ten 2 mm thick uncoated quartz plates. The angle between the electric vector of the dissociation laser E_{diss} and the propagation direction of the probe laser k_{probe} could be changed by rotating E_{diss}.

During an experiment, the pressure of the reaction chamber was $(1\text{–}10)\times 10^{-5}$ Torr. The detection chamber was separated from the main chamber by a meshed screen slit and was pumped differentially by a liquid N_2-trapped diffusion pump. Ions were detected by an electron multiplier. The output of the detector was amplified and fed into a boxcar averager.

The Doppler profiles of Cl($^2P_{3/2}$) and Cl*($^2P_{1/2}$) were measured using (2+1) resonance-enhanced multiphoton ionization (REMPI). The bandwidth of the probe laser was reduced to 0.1 cm^{-1} by means of an intracavity etalon in the dye laser. The two-photon resonance absorptions used for this process were $4p\ ^2D_{3/2} \leftarrow 3p\ ^2P_{3/2}$ at 235.3 nm and $4p\ ^2D_{3/2} \leftarrow 3p\ ^2P_{1/2}$ at 237.8 nm.

The Doppler profiles of H fragments were also measured by the REMPI method. The bandwidth of the probe laser in this case was 0.4 cm^{-1}. The resonance step for this process was the two-photon transition $2s\ ^2S \leftarrow 1s\ ^2S$ at 243.135 nm. The relative MPI sensitivities of H and Cl detection were determined by photodissociating HCl at 193 nm. Under the same experimental conditions, we found that the signal sensitivity ratio $I(\text{H})/I(\text{Cl})$ was 4 ± 1 for HCl.

B. Angular distribution measurement by perfect focusing mass spectroscopy

Angular distributions of Cl (Cl*) photofragments were measured at 235.3 and 237.8 nm by REMPI of the Cl photofragments in the "one-color" photodissociation of chloroethylenes with a perfect focusing mass spectrometer. Our homemade mass spectrometer used to obtain mass spectra and angular distributions is identical to that reported previously.[20] Briefly, the polarized light pulse from an excimer-pumped dye laser was focused into an effusive beam of sample gases by a 150 mm lens in order to dissociate the parent molecules and also to ionize the chlorine atomic photofragments. The effusive beam emerged from a 0.3 mm diameter needle. The vacuum chamber was evacuated by a diffusion pump to a base pressure of 10^{-6} Torr.

By means of a canonical transformation, Iwata[21] has shown that a perfect three-dimensional focusing field is realized by the use of a combination of an electrostatic and a uniform magnetic field. Once the ions are scattered from the interaction point of the molecules and the focused laser light, all charged particles of the same effective mass converge perfectly to a focusing point (detection point) independent of the initial velocity vector. Mass spectra were obtained by changing the electric field strength. For the measurement of angular distributions, a conical collimator was placed in front of the detector. The collimator tube had a 0.7 mm diameter and a length of 2.0 mm, which gave the detector (Spiraltron, Galileo) a 10° field of view. The angular distribution was obtained by rotating the electric vector of the laser light with respect to the effective detector direction.

C. Intensity dependence of the photofragments

The apparatus used to measure the intensity dependence of the product yields has been reported previously.[9,22] Briefly, it consists of a two-chamber pulsed molecular beam apparatus equipped with a shuttered time-of-flight (TOF) mass spectrometer. The parent molecules were introduced into the apparatus through a pulsed valve (Newport, BV100) having a 0.5 mm orifice. The backing pressure was typically 100 Torr of neat gas. Variation of this pressure showed no evidence of clustering. The molecules were photolyzed with an ArF laser (Lambda Physik EMG 150) and detected by 2+1 REMPI using a frequency doubled dye laser (Lambda Physik EMG 102/ FL 2002). The time delay between the pump and probe lasers was typically 500 ns for Cl^+ and HCl^+ and 100 ns for H^+. Since HCl^+ ion is a major product, it was necessary to shutter the detected beam to prevent the channel plate detector from saturating. This was accomplished by biasing one of the XY deflection plates to deflect unwanted ions and grounding the plate to pass the mass of interest.

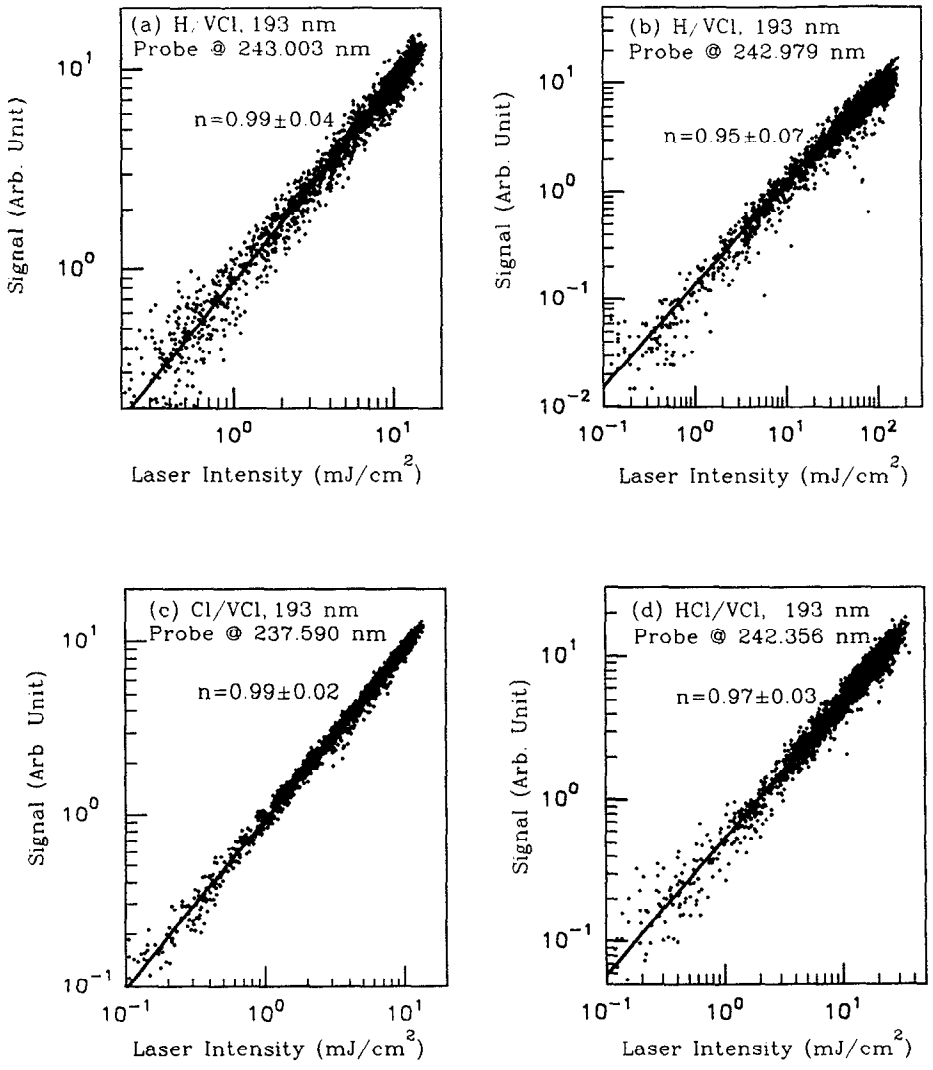

FIG. 1. Intensity of REMPI signals from (a) and (b) H; (c) Cl; and (d) HCl as functions of the fluence of the photolysis laser. The data in panels (a), (c), and (d) were taken with an unfocused ArF laser, while panel (b) was recorded using a mildly focused laser. The wavelengths of the probe laser are recorded in each panel. The straight lines are least-squares log–log fits. The uncertainties are single standard deviations.

The power dependence of the product yields was determined by attenuating the pump laser with an absorption cell filled with ammonia gas. During a run, the cell was evacuated slowly while product peaks were captured for each laser pulse with a multichannel boxcar detector. By this method, it was possible to obtain a power spectrum with a variation in photolysis intensity of two to three orders of magnitude in just five minutes.

III. RESULTS

A. Intensity and pressure dependence of the product yields

Figure 1 shows the intensities of the H, Cl, and HCl signals as functions of the fluence of the photolysis laser. The data in panels 1(a), 1(c), and 1(d) were taken with an unfocused beam, while in panel (1b) the photolysis laser was focused mildly with a 50 cm lens. In the case of H atoms, intensity measurements were made both at the center of the Doppler profile {243.003 nm [panel (1a)]} as well as at the blue wing {242.981 nm [panel (b)]}. In every case, a log–log plot of signal vs laser energy has a slope of unity.

Figure 2 shows the power dependence of HCl^+ ions produced from expansions of vinyl chloride (VCl) and neat HCl using a focused ($f=38$ cm) 193 nm laser beam to ionize the parent molecules. The signals have been normalized by the backing pressure in the nozzle. The HCl^+ signal produced from VCl has a slope of 3 for fluences between 2 and 25 mJ/cm^2 and a slope of 2 between 25 and 500 mJ/cm^2. Increasing the VCl pressure fivefold resulted in a linear increase in signal at all fluences, showing that the curvature above 1 J/cm^2 is not an instrumental effect. The HCl^+ signal produced from HCl has a slope of 2 between 100 and 500 mJ/cm^2 and levels off at higher fluences. In the region where both signals have slopes of 2, the HCl^+/VCl signal is approximately 100 times larger than

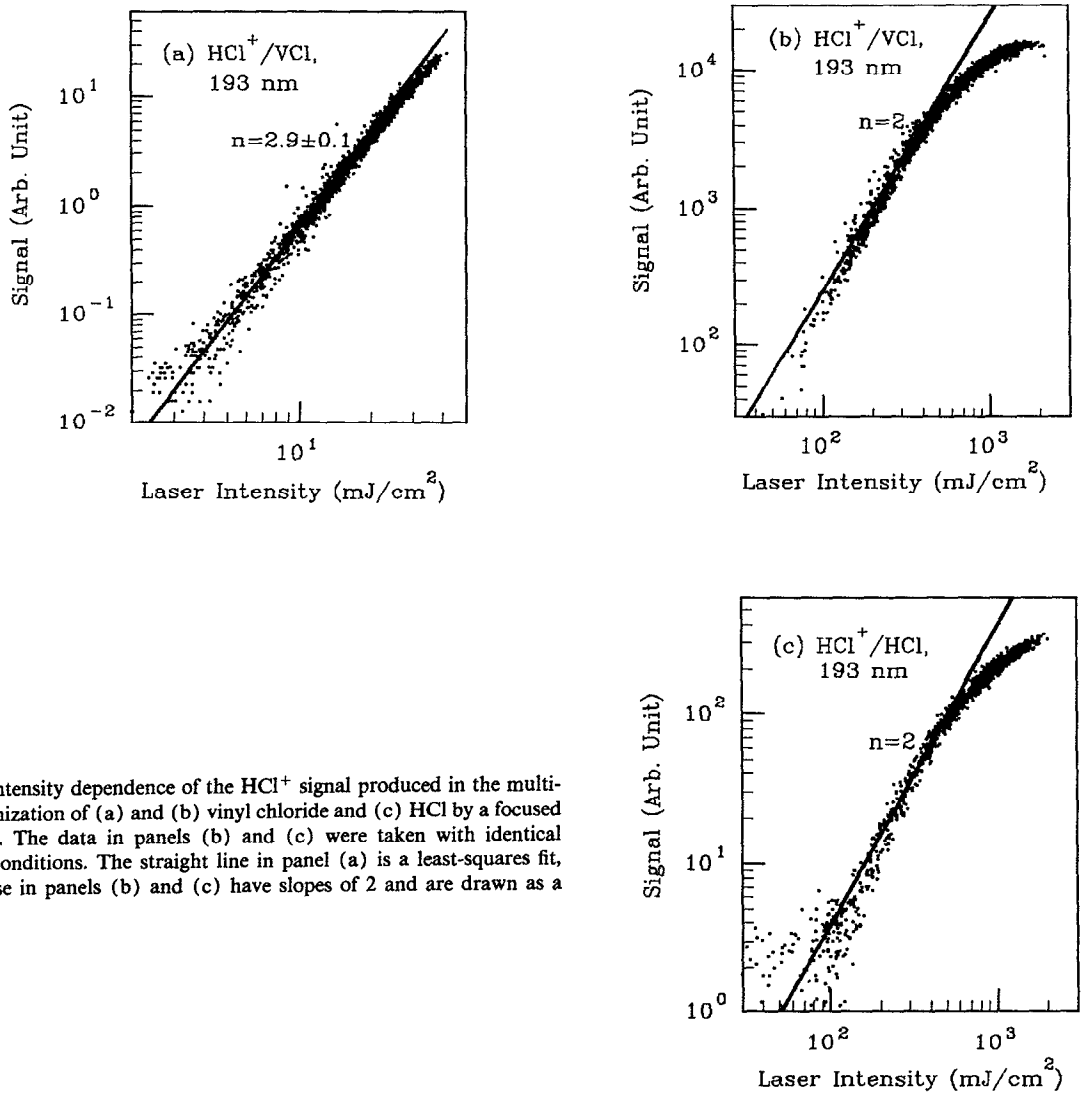

FIG. 2. Intensity dependence of the HCl^+ signal produced in the multiphoton ionization of (a) and (b) vinyl chloride and (c) HCl by a focused ArF laser. The data in panels (b) and (c) were taken with identical focusing conditions. The straight line in panel (a) is a least-squares fit, while those in panels (b) and (c) have slopes of 2 and are drawn as a reference.

the HCl^+/HCl signal, while at saturation, we estimate the ratio to be approximately 30:1.

In another experiment, we compared the saturated yields of HCl^+ and Cl produced from VCl. We estimate the ratio to lie between 10^{-2} and 10^{-3}. Despite repeated attempts, we did not observe any parent vinyl chloride ions.

In the course of these experiments, we also determined the absorption cross section of HCl at 193 nm by measuring the transmission of the unfocused laser beam through a cell containing known pressures of HCl. The value we obtained is $(8.1\pm0.4)\times10^{-20}$ cm^2. This result is in excellent agreement with the value of 8.26×10^{-20} interpolated from the data of Inn[23] and in clear disagreement with the earlier value of Myer and Samson.[24]

Because a large amount of HCl^+ is produced from vinyl chloride with an unfocused pump laser, the possibility exists that the charge exchange reaction

$$HCl^+ + C_2H_3Cl \rightarrow HCl + C_2H_3Cl^+ + 2.7 \text{ eV}, \quad (5)$$

followed by fragmentation of the organic ion, could produce neutral HCl in competition with unimolecular elimination [reaction (4)]. Another possible bimolecular process is the reaction of hot Cl atoms [produced in reaction (3)] with the parent molecule

$$Cl + C_2H_3Cl \rightarrow HCl + C_2H_2Cl. \quad (6)$$

Both of these processes are likely to have large cross sections and therefore could occur under the nominally "collisionless" conditions of the molecular beam. To test for this possibility, we varied the pressure in the beam by an order of magnitude. We found that the Cl and HCl yields have the same density dependence. Since it is generally agreed that Cl detachment is unimolecular, we are confident that bimolecular reactions did not occur under our experimental conditions.

B. Angular distributions of the Cl photofragments from dichloroethylenes at 235–237 nm by a perfect focusing mass spectrometer

Since dichloroethylenes absorb strongly in the UV region, photodissociation and chlorine atom detection can be achieved in a single color experiment using 235.3 nm to

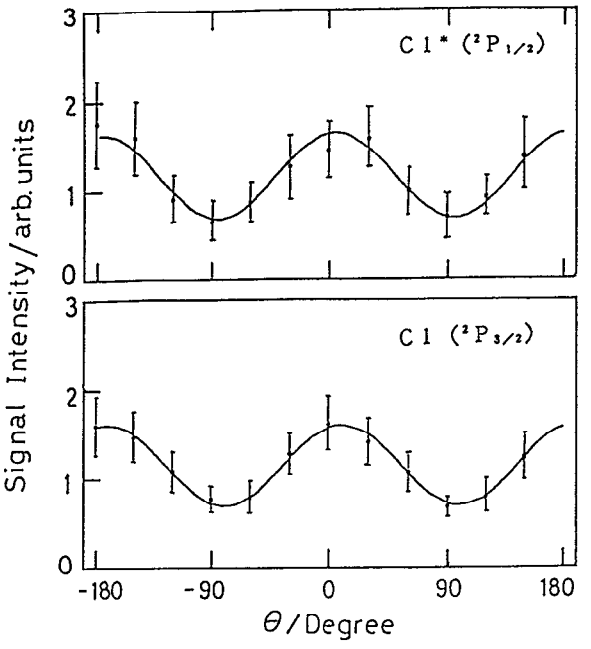

FIG. 3. Examples of the angular distributions of chlorine atom photofragments from the photodissociation of *t*-CHClCHCl. The upper panel is the signal from $Cl^*(^2P_{1/2})$ with a dissociation wavelength of 235.3 nm, while the lower panel is for $Cl(^2P_{3/2})$ at 237.8 nm. θ is the angle between the detection axis and the direction of the electric vector of the dissociation laser. The smooth curves are given by Eq. (7) with $\beta=0.6$

detect $Cl(^2P_{3/2})$ and 237.8 nm for $Cl^*(^2P_{1/2})$. The intensity of Cl^+ was measured as a function of the angle θ between the detection axis and the direction of the electric vector of the dissociation laser in the perfect focusing mass spectrometer. An example is shown in Fig. 3 for *t*-$C_2H_2Cl_2$. The experimentally obtained angular distribution is analyzed assuming the center-of-mass angular distribution $f(\theta)$,[25]

$$f(\theta)=[1+\beta P_2(\cos\theta)]/4\pi, \quad (7)$$

where $P_2(\cos\theta)$ is the second-order Legendre polynomial. In order to avoid distortion of the anisotropy by saturation, the laser power was reduced until the β value reached an asymptotic value. The smooth curves in Fig. 3 are a least-squares fit of Eq. (7) to the data. The β value for *t*-CHClCHCl was 0.65 ± 0.08. Other sets of data for CH_2CCl_2, $CHClCCl_2$, and C_2Cl_4 are summarized in Table I. These values are in good agreement with Umemoto's values. Although their dissociation wavelength (193 nm) is different from ours (235–238 nm), it appears that the electronic transition of the dichloroethylenes is the same (π,π^*). Although they could not separate Cl* from Cl in their time-of-flight spectra, its contribution is at most only 23%, as will be discussed below. Taking averaged values of both experiments, the anisotropy parameters are 0.64 for Cl detachment from *t*-CHClCHCl and -0.20 from CH_2CCl_2.

Chlorine atom fragments from CH_2CCl_2, CCl_2CHCl, and C_2Cl_4 have low β values. β is given by $2P_2(\cos\chi)$, where χ is the angle between the transition dipole moment

TABLE I. Anisotropy parameters for angular distribution of Cl photofragments from dichloroethylenes at 235–237 nm.

		β	
Parent molecule	Species	This work	Umemoto *et al.*[b]
t-CHClCHCl	Cl	0.65 ± 0.08	0.63 ± 0.02
	Cl*	0.61 ± 0.06	···
CH_2CCl_2	Cl	-0.15 ± 0.01	-0.24 ± 0.016
	Cl*	-0.09 ± 0.01	···
CCl_2CHCl	Cl	-0.05 ± 0.01	···
CCl_2CCl_2	Cl	-0.07 ± 0.01	···

[a] $Cl(^2P_{3/2})$ atoms detected at 235.3 nm and $Cl^*(^2P_{1/2})$ atoms at 237.8 nm.
[b] Reference 1.

and the direction of recoil of the Cl photofragment from the carbon atom. Since CCl_2CHCl and C_2Cl_4 have (π,π^*) transition moments which lie on the C–C axis,[1] χ is close to the magic angle (54.7°), and hence β is close to zero.

C. Doppler profiles and branching ratios of chlorine and hydrogen atoms

Doppler profiles of $Cl(^2P_{3/2})$ and $Cl^*(^2P_{1/2})$ from photodissociation of vinyl chloride and dichloroethylenes at 193 nm are shown in Fig. 4. Because the $Cl^*(^2P_{1/2})$ signal intensity for the dichloroethylenes was almost an order of magnitude smaller than that of $Cl(^2P_{3/2})$, the Doppler profiles of $Cl^*(^2P_{1/2})$ could not be measured with the narrow bandwidth probe laser. Figure 5 shows the Doppler profiles of the H fragments from vinyl chloride and dichloroethylenes at 193 nm.

We also measured the signal intensity ratio $I(Cl^*)/I(Cl)$ for vinyl chloride and *t*-CHClCHCl. For vinyl chloride, it is 0.12 ± 0.02 (one standard deviation), which is in good agreement with the result of 0.122 (±0.003) reported by Reilly *et al.*[9] For *t*-CHClCHCl, it is 0.06 ± 0.01, while for CH_2CCl_2, it is 0.11 ± 0.02. In an independent calibration,[26] we determined the detection sensitivity ratio $S(Cl^*)/S(Cl)=2.5$, from which we obtain the branching ratios for [Cl*]/[Cl] listed in Table II.

The relative yield of [Cl]/[H] was determined to be 4 ± 1 for the photodissociation of CH_2CCl_2. For *t*-CHClCHCl and CCl_2CClH, we could not obtain the relative yield [Cl]/[H] under the same experimental conditions, but we can safely say that the ratios are greater than 10.

While we did not measure in the present study the relative yields of Cl to HCl, previous results[1,2,4,11] (listed in Table II) indicated that they are comparable. The scatter among the reported ratios cannot be attributed to differences in light sources, since the discrepancy between the studies using a 193 nm laser[1,4] is greater than that between the laser and lamp results. One possible cause of the scatter is the occurrence of reaction (5) or (6) under bulk conditions.

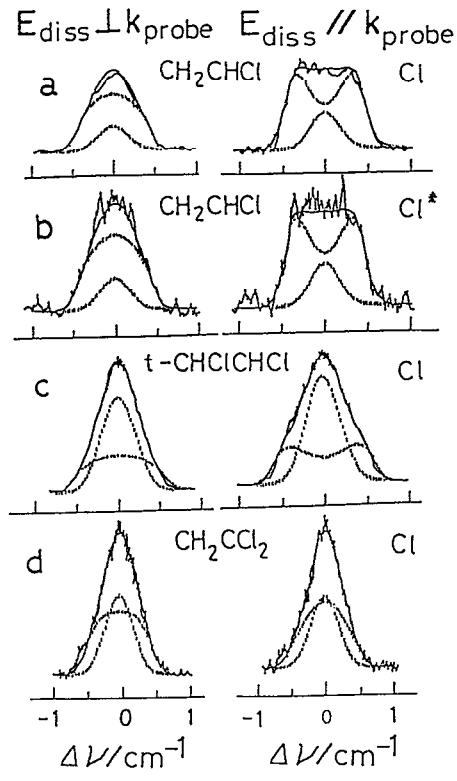

FIG. 4. Doppler profiles of chlorine atom fragments from the photodissociation of chloroethylenes at 193 nm. The traces are for (a) $Cl(^2P_{3/2})$ obtained from CH_2CHCl; (b) $Cl^*(^2P_{1/2})$ from CH_2CHCl; (c) $Cl(^2P_{3/2})$ from *t*-CHClCHCl; and (d) $Cl(^2P_{3/2})$ from CH_2CCl_2. The abscissa is the two-photon detuning of the probe laser. The left-hand column corresponds to a laser alignment with the polarization vector of the dissociation laser perpendicular to the propagation axis of the probe laser, while on the right they are parallel to each other. The smooth curves are simulations. Contributions of the lower and higher energy components to the Doppler profiles are shown separately. Their ratios are 0.24, 0.7, and 1.4 for CH_2CHCl, *t*-CHClCHCl, and CH_2Cl_2, respectively. The lower energy component has $\beta=0$. The β values of the higher energy components are the averages of those obtained from our angular distributions and those reported in Ref. 1. The values are 0.85 for CH_2CHCl, 0.64 for *t*-CHClCHCl, and -0.20 for CH_2CCl_2.

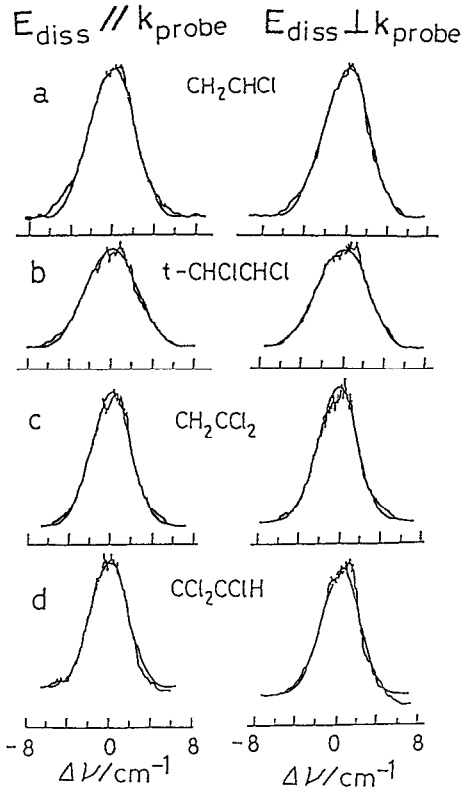

FIG. 5. Doppler profiles of hydrogen atom photofragments from the photodissociation of chloroethylenes at 193 nm. The traces correspond to (a) CH_2CClH; (b) *t*-CHClCHCl; (c) CH_2CCl_2; and (d) CCl_2CClH. The abscissa is the two-photon detuning of the probe laser for the $H(2s\,^2S)$–$H(1s\,^2S)$ transition. The smooth curves are simulations assuming Maxwell–Boltzmann translational energy distributions with the average energies listed in Table II. The left-hand column corresponds to a laser alignment with the polarization vector of the dissociation laser perpendicular to the propagation axis of the probe laser, while on the right they are parallel to each other.

IV. KINETIC MODELING

In this section we present models for simulating the Doppler profiles and energy dependence of the products.

A. Simulation of the Doppler profiles

The Doppler profile of the fragments results from a projection of the fragment velocity distribution onto the propagation direction of the probe laser k_{probe}, i.e., along the *z* axis. The velocity distribution along the *z* axis is given by

$$g(v_z)=\int_{v>|v_z|} f(v)[1+\beta P_2(\cos\alpha)P_2(v_z/v)]/v\,dv, \qquad (8)$$

where $f(v)$ is the fragment velocity distribution. Replacing $v_z=c\Delta\nu/\nu_0$ in Eq. (8), one obtains the Doppler profile of the fragment.[27]

Umemoto *et al.*[1] reported two different energy distributions for Cl atoms produced in the photodissociation of dichloroethylenes, corresponding to high and low energy peaks in their time-of-flight spectra. There is also a hint of a low energy component in their vinyl chloride spectrum. If there are two different processes for Cl detachment, one might expect different anisotropy parameters for the two pathways. In our simulation of the Doppler profiles, poor agreement with the data was obtained if we assumed a unimodal velocity distribution with a single anisotropy parameter. Excellent agreement is obtained, however, if we assume a bimodal distribution. In this fit, the β values of

TABLE II. Product branching ratios.

Molecule	[Cl*]/[Cl]	[Cl]/[H]	[Cl]/[HCl]
CH_2CHCl	0.30±0.05	···	0.50,[a] 1.1,[b] 0.48,[c] 1.4[d]
t-CHClCHCl	0.15±0.03	>10	1.04[a], 2.2[b,e]
CH_2CCl_2	0.28±0.05	4±1	0.79[a]
CCl_2CHCl	···	>10	2.9[a]

[a]Reference 2.
[b]Reference 1.
[c]Reference 4.
[d]Reference 11.
[e]The value for the *cis* isomer is 3.5.

TABLE III. Ratio of the concentrations of low and high translational energy components of the Cl atom fragments from photodissociation of vinyl chloride and dichloroethylenes at 193 nm.

Molecule	Ratio	
	This work	Umemoto *et al.*[a]
CH_2CClH	0.24	0.0
CH_2CCl_2	0.7	0.8
t-CHClCHCl	1.4	1.4

[a]Reference 1.

the low energy component are assumed to be zero, while the β values of the higher energy component are obtained from our perfect focusing mass spectroscopic measurement and the data of Umemoto *et al.*[1] These values are 0.85 for CH_2CHCl, 0.64 for *t*-CHClCHCl, and -0.20 for CH_2CCl_2.

A sufficient condition for obtaining $\beta=0$ for the low energy component is that the excited parent molecule lives long compared with the rotational period. Assuming that this is the case, the translational energy distribution $P(E_t)$ for the atomic fragments are given by the Zamir–Levine statistical model[28]

$$P(E_t) \propto E_t^{1/2}(E_{\text{avl}}-E_t)^{s+1/2}. \tag{9}$$

In deriving Eq. (9), it is assumed that (a) all isoenergetic quantum states of the products are equally populated and (b) that a simple harmonic approximation describes the vibrational density of states.[28] For this distribution, the average fraction f_t of available energy transforming into translational energy is given by

$$f_t=3/2\ (s+3), \tag{10}$$

where s is the number of vibrational degrees of freedom in the organic fragment radical. In our case, $s=9$ is assumed for vinyl chloride and dichloroethylenes. The available energy at 193 nm was taken to be 59 kcal/mol.

The translational energy distribution function of the high energy Cl atoms was arbitrarily assumed to have a Gaussian form i.e.,

$$P(E_t) \propto \exp[-(E_t-E_{\text{peak}})^2/E_\sigma^2], \tag{11}$$

where E_{peak} represents the peak position of the high energy components of Umemoto's data,[1] namely 26 kcal/mol for vinyl chloride and *t*-dichloroethylene and 17.5 kcal/mol for gem dichloroethylene. The value of E_σ was found by fitting Eq. (11) to the high energy component of Umemoto's data. For vinyl chloride and *trans*-dichloroethylene, $E_\sigma=10$ kcal/mol was obtained, while for gem dichloroethylene $E_\sigma=12$ kcal/mol was obtained.

To simulate the Doppler profiles, the ratio of the low to high energy components was treated as a free parameter. Figure 3 shows the best fit curves. Table III lists the intensity ratios of the low energy component to the high one. We found that the $Cl^*(^2P_{1/2})$ Doppler profile for vinyl chloride can be fit by the same β values and translational energy distribution as $Cl(^2P_{3/2})$. These ratios are in good agreement with the results obtained by Umemoto *et al.*[1] except for vinyl chloride.

TABLE IV. Average translational energy of the hydrogen atom photofragment.

Molecule	$\langle E_t\rangle$[a] (kcal/mol)	E_{avl}[b] (kcal/mol)	$\langle E_t\rangle/E_{\text{avl}}$	s[c]
CH_2CHCl	17	49	0.35	1
t-CHClCHCl	18	49	0.37	1
CH_2CCl_2	13	49	0.27	3
CCl_2CHCl	12	50	0.24	3

[a]Average translational energy. Error bars are ± 2 kcal/mol.
[b]Available energy, based on $D_0(\text{C–H})=100$ kcal/mol and a vibrational energy of 2 kcal/mol for CCl_2CClH and 1 kcal/mol for the other molecules.
[c]The effective number of vibrational degrees of freedom. For $s=1$, the α model predicts $\langle E_t\rangle/E_{\text{avl}}=0.38$; for $s=3$, it predicts $\langle E_t\rangle/E_{\text{avl}}=0.25$.

We turn finally to the H atom fragments. In this case, the Doppler profiles are well represented by an isotropic angular distribution and by a Maxwell–Boltzmann translational energy function. Table IV lists the average translational energies obtained from the Doppler profiles.

B. Intensity dependence

Consider the following model for two-photon ionization of HCl:

$$\text{HCl}+h\nu \xrightarrow{k_1} \text{HCl}^*, \tag{12a}$$

$$\text{HCl}^*+h\nu \xrightarrow{k_2} \text{HCl}^+, \tag{12b}$$

where in general the rate constants k_1 and k_2 are proportional to I^{n_1} and I^{n_2}. Solution of the rate equations gives the familiar result[29]

$$(\text{HCl}^+)/(\text{HCl})_0=1-[k_1/(k_1-k_2)]\exp(-k_2t) + [k_2/(k_1-k_2)]\exp(-k_1t), \tag{13}$$

where t is the duration of the laser pulse. In the low fluence limit, where both k_1t and k_2t are $\ll 1$, the yield [the right-hand side of Eq. (13)] becomes $\frac{1}{2}k_1k_2t^2$, which is proportional to $I^{n_1+n_2}$. If the first step is saturated (i.e., $k_1t\gg 1$), the yield is k_2t, while if the second step is saturated, the yield is k_1t.

We can easily expand the kinetic model to include three or more steps. For three steps, the yield is the sum of three exponentials. In the low fluence limit, it is simply $k_1k_2k_3t^3/6$. If, e.g., the first step is saturated, the yield reduces to $\frac{1}{2}k_2k_3t^2$.

We can further generalize the model to include fluorescence and dissociation. Fluorescence has the effect of coupling the rate constants so that the eigenvalues become nonlinear combinations of the rate constants. Adding a dissociation step to the three level model, e.g.,

$$\text{HCl}^*+h\nu \xrightarrow{k_d} \text{H}+\text{Cl}, \tag{12c}$$

changes the yield to

$$(HCl^+)/(HCl)_0 = k_2/k_2' - [k_1/(k_1-k_2')] \times (k_2/k_2')\exp(-k_2't) + [k_2/(k_1-k_2')]\exp(-k_1t), \quad (14)$$

where $k_2' = k_2 + k_d$. In the high fluence limit, where k_1t and $k_2't$ are both $\gg 1$, the yield drops from unity in Eq. (13) to k_2/k_2' in Eq. (14). In the low fluence limit, the result is still $\frac{1}{2}k_1k_2t^2$.

V. DISCUSSION

A. Chlorine atom detachment

Both our experiment and that of Umemoto *et al.*[1] reveal the existence of low and high energy chlorine atoms, with most of the Cl atoms belonging to the latter component. In addition, we found that the β values that we measured at 235–238 nm and Umemoto *et al.* reported at 193 nm are approximately equal. A number of questions arise from these findings. First, do the two energy components result from two different electronic transitions induced by the photon, or is there only one primary transition followed by subsequent decay into different product channels? Second, how can we rationalize the observation of the same β values for two different photon energies? And, finally, can we identify the electronic mechanisms that produce the two energy components?

We will address first the question of one vs two transitions. It is generally agreed that for ethylenic compounds, the strongest absorption is due to a (π,π^*) transition, which for vinyl chloride has a peak oscillator strength of 0.4.[30] It is also accepted that the primary dissociative state for producing Cl atoms is the (n, σ^*) state. Since the oscillator strength for that state is very small,[2] it follows that the most likely mechanism for producing the major component (i.e., the high energy component) of Cl atoms is by internal conversion from the initially prepared (π,π^*) state. It is probable that internal conversion is also responsible for producing the low energy component for two reasons. First, there are no other transitions in this energy region likely to have a large enough oscillator strength. Second, and more important, all the molecules we studied had the same β value for the low energy component, namely $\beta=0$. It is hard to see why a direct transition would have the same anisotropy for all of the molecules studied, unless the product results from a long-lived state.

We consider next the variation of β with wavelength. The average energy of the Cl atom in the low energy component is approximately 10 kcal/mol for all of the compounds studied, implying that for this channel, the organic fragment must be highly excited. The photon energy at 235–238 nm is 27 kcal/mol less than at 193 nm. Since at the longer wavelength there is insufficient energy to produce such highly excited fragments, we may suppose that this channel is closed at 235–238 nm. In the case of Umemoto's experiment at 193 nm, the configuration of their apparatus reduced its sensitivity for slowly moving atoms. It follows, therefore, that both experiments detected primarily the high energy component of the Cl atoms.

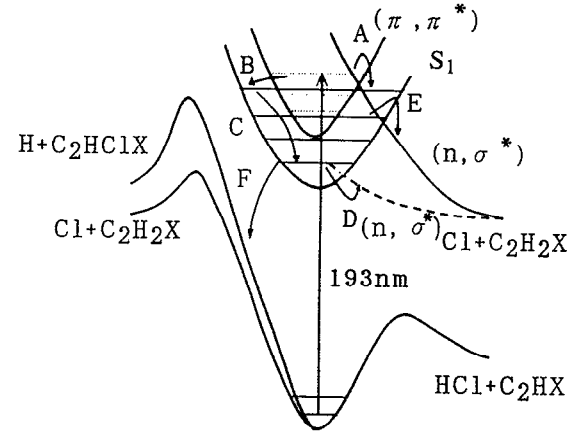

FIG. 6. A schematic of cuts along the dissociation and elimination coordinates for the multidimensional potential energy surface of chloroethylenes. Process A is a curve crossing from the intially excited $\pi\pi^*$ state to the higher antibonding $n\sigma^*$ state. Process B is an internal conversion to the lowest excited bound singlet state, labeled S_1. Process C is internal redistribution of energy in the long-lived state. Processes D and E are curve crossings to antibonding $n\sigma^*$ states. Process F is a radiationless transition to the ground potential energy surface. Dissociation on the $n\sigma^*$ surface produces Cl atoms. Dissociation on the lowest surface produces H, HCl, and low energy Cl. Absorption of a second photon may also occur following process B.

Since the (π,π^*) transition extends over this wavelength range, it is reasonable that the same anisotropy should have been observed in the two experiments.

We turn last to the electronic mechanism for producing two energy components. In the photodissociation of C_2H_3Br at 193 nm, Wodtke and Lee[15] observed a low energy tail in the time-of-flight spectrum of the vinyl radical, which they assigned to the $C_2H_3(\tilde{A})$ state. Based on their data, they deduced a heat of formation of 113.5 ± 1.5 kcal/mol for this state and used this value to reassign the spectrum reported by Hunziker *et al.*[31] This heat of formation gives an available energy of 15 ± 2 kcal/mol for the low energy Cl atom in the photodissociation of vinyl chloride at 193 nm. Since this energy is only 8–10 kcal/mol greater than the peak energies reported by Umemoto *et al.* for the low energy component of Cl, it is plausible that this channel results from the production of an electronically excited vinyl radical. A difficulty with this explanation is that the peak kinetic energy of the low energy Cl atom would then be approximately half of the total available energy, which is inconsistent with energy partitioning of a long-lived (isotropic) precursor.

We consider an alternate mechanism, which is illustrated in Fig. 6. We will designate the lowest lying bound excited state as S_1. Umemoto *et al.* found in their calculations that the lowest excited singlet state is the (π,σ^*), which they presumed to be bound. While additional theoretical work is needed to determine whether the (π,σ^*) state is indeed bound, we may nevertheless suppose that the S_1 state lies in this energy range. Umemoto *et al.* proposed that internal conversion to this state (process B in Fig. 6) followed by a radiationless transition to the ground

state (process F) is the mechanism for producing HCl. We suggest that this intermediate state may also be the long-lived precursor for generating the isotropic, low energy Cl atoms.

For the dichloroethylenes, *ab initio* calculations[1] show that there are two repulsive (n,σ^*) states, while for vinyl chloride, there is only one such unbound state. In the dissociation process, population in the (π,π^*) state is transferred to the S_1 state by internal conversion (process B in Fig. 6). We propose that the direct crossing of (π,π^*) to the higher (n,σ^*) state produces the high energy component of the Cl fragment (process A), while the crossing of S_1 to the lower (n,σ^*) produces the lower energy component (process D). Since the higher (n,σ^*) state can also cross S_1, this crossing can also produce the lower energy component of the Cl fragment (process E). Still another possible mechanism for producing low energy Cl is a radiationless transition to the ground state (process F) followed by dissociation on this surface.

B. Hydrogen atom detachment processes

Our observation of a linear intensity dependence of the H atom yield is indicative of a single-photon process. In order to check the possibility that some high energy atoms may be produced by a two-photon process (either by absorption of two photons by the parent molecule or by sequential H atom elimination), we measured the intensity dependence of the blue wing of the Doppler profile [Fig. 1(b)]. Our observation of a unit slope for fluences as high as 100 mJ/cm^2 shows that these atoms are also produced by a single photon, obtaining their "superthermal" energy from internal energy of the parent molecule. While at still higher fluences one would expect to observe secondary photodissociation of the CH_2CCl radical, under our conditions the very high absorption rate of the parent molecule is apparently much faster than subsequent absorptions.

The C–H bond energies for the chloroethylenes have not been reported. However, the C–H bond dissociation energy for ethylene is reported to be 107–110 kcal/mol.[7] The effect of chlorination is to reduce the C–H bond energy. For example, D_0(C–H) for CH_4, CH_3Cl, CH_2Cl_2, and $CHCl_3$ is 104, 101, 99 and 96 kcal/mol, respectively.[32] For the chloro-olefines, there is an additional stabilization caused by interaction of one of the Cl nonbonding orbitals with the C=C π orbital. Taking this effect into account, we estimate that D_0(C–H) for the chloroethylenes is 100 kcal/mol.

Based on this assumed value of D_0, we calculated the partition of available energy E_{avl} between translational and internal degrees of freedom. Table IV lists the average translational energy $\langle E_t \rangle$ and the fraction $f_t = \langle E_t \rangle / E_{avl}$. This fraction lies between 24% and 35%. This is considerably larger than is typically observed for the photodetachment of H atoms from large molecules,[33] and is indicative of a nonstatistical distribution of the available energy between the vibrational modes of the molecule.

From the internal energy E_{int} of the organic radical, we can calculate an effective rovibrational temperature T_v from the equation

$$E_{int} = \sum_i \{h\nu_i / [\exp(h\nu_i / kT_v) - 1]\} + (3/2)kT_v , \qquad (15)$$

where the sum is over all vibrational modes of the radical. The results are listed in Table V for H atom detachment and in Table VI for the low energy Cl product. For H atoms we find that the translational temperature T_t is two to three times greater than T_v, while for Cl it is 20% to 25% lower. The result for H is surprising since the isotropic Doppler profile indicates that detachment takes longer than a rotational period. This seeming contradiction may be explained if vibrational equilibration is much slower than detachment, so that only a few vibrational modes are active. A plausible mechanism therefore is that H atom elimination occurs on the ground electronic surface following internal conversion from the (π,π^*) surface. This happens on a time scale that is slow compared with rotation, but fast compared with vibrational thermalization.

TABLE V. Rovibrational temperature of the radical fragment $T(R)$ and the translational temperature of the H fragment T_t(H) for H detachment.[a]

Molecule	$T(R)$	T_t(H)
CH_2CHCl	2200	5700
t-CHClCHCl	1900	6700
CH_2CCl_2	2200	4400
CCl_2CClH	2100	4400

[a]Temperatures are in degrees Kelvin.

An important characteristic of the C–H bond is the fact that the mass of the H atom is very small compared with that of the organic fragment. Such a C–H detachment process may have little effect on atoms not bonded to the same C atom. We designate the carbon atom in this bond as the α carbon. We propose a mechanism, called the "α model," in which we assume that only atoms bonded to the α carbon actively participate in sharing energy with the departing H atom. This model provides an upper bound to f_t by assuming that all of the available energy is localized on the α carbon. We continue to use Eq. (9) to describe the energy distribution, but now s denotes the number of vibrational degrees of freedom of only the participating atoms. Three possible cases are

$$\begin{aligned} &-C\equiv C-H, && s=1, && f_t=0.38; \\ &\gtrdot C=C-H, && s=3, && f_t=0.25; \\ &\gtrdot C-H, && s=6, && f_t=0.17. \end{aligned} \qquad (16)$$

TABLE VI. Rovibrational temperature of the radical fragment $T(R)$ and the translational temperature of the Cl, T_t(Cl), fragment for the channel producing low energy Cl atoms.

Molecule	$T(R)$	T_t(Cl)
CH_2CHCl	3400	2500
t-CHClCHCl	3100	2500
CH_2CCl_2	3200	2500

[a]Temperatures are in degrees Kelvin.

From Table IV, we see that for CCl_2CHCl and CH_2CCl_2 agreement of the experimental results with the α model is good. For CH_2CHCl and CHClCHCl, however, we find that $\langle E_t\rangle/E_{avl}$ corresponds to $s=1$. This means that even atoms connected to the α atom do not participate completely in the energy distribution for these two molecules. While the α model is an oversimplification, it provides a rationale for nonstatistical partitioning of energy.

There are several examples in the literature which can also be rationalized with the α model. Recently, Jackson *et al.* [34] reported the translational energy distribution of the H atom produced in the photodissociation of allene (C_3H_4) at 193 nm. The maximum translational energy of the H atom was found to be 36.4 kcal/mol. Taking $E_{avl}=36.4$ kcal/mol and $s=3$, the α model predicts an average translational energy of 9.1 kcal/mol, which is in good agreement with the experimental value of 8.95 kcal/mol.

Tonokura *et al.*[35] reported the average translational energy of H atoms produced in the photodissociation of saturated hydrocarbons at 157 nm. The available energy for H detachment from C_3H_8, n-C_4H_{10}, and n-C_6H_{14} is approximately 97 kcal/mol. According to the α model, $s=6$ and $f_t=17\%$. The average translational energy is therefore calculated to be 16 kcal/mol, which is in good agreement with the experimental value of 14 kcal/mol.

C. Molecular elimination processes

Our observation of a linear energy dependence for the production of HCl is consistent with the mechanism proposed by Umemoto *et al.*,[1] namely single-photon excitation of the the $\pi\pi^*$ state followed by a radiationless transition to the ground state (processes B, C, and F) and decomposition on the lowest surface. Our present measurements do not distinguish between three-center ($\alpha\alpha$) and four-center ($\alpha\beta$) elimination, which will be the subject of a future study.

We turn now to the three-photon production of the HCl^+ ion. A mechanism proposed by Rossi and Helm[4] is one-photon elimination of neutral HCl followed by two-photon ionization of HCl. A difficulty with this mechanism is that they were unable to ionize HCl in a molecular beam even with a focused 193 nm laser. They rationalized this discrepancy by assuming that HCl ($v=0$) in the molecular beam dissociates rapidly on the $A(^1\Pi)$ surface and does not have a chance to absorb a second photon. In contrast, HCl produced by photoelimination from VCl is vibrationally excited. Rossi and Helm proposed that HCl ($v''=10$) undergoes a one-photon resonant transition to the $V(v=0)$ state, followed by absorption of a second photon to produce HCl^+. This mechanism is easily ruled out on two grounds. First, the $X(v''=10)\rightarrow V(v'=0)$ transition is not resonant at 193 nm. The term energy is 52 156 cm^{-1},[36] while the energy provided by the laser lies between 51 745 and 51 820 cm^{-1} [full width at half-maximum (FWHM)].[37] Second, the Franck–Condon factor for this transition is approximately 10^{-5},[38] which is two to three orders of magnitude smaller than our estimate of the quantum yield.

A variant of the Rossi–Helm mechanism which we must consider is 1+1 MPI of HCl, resonantly enhanced by the A state. While it is true that dissociation of the A state is rapid, this effect may be more than offset by resonance enhancement of the two-photon cross section. Since the one-photon absorption cross section of $HCl(v=1)$ is ten times greater than that for $HCl(v=0)$,[39–41] an overall enhancement of two orders of magnitude is conceivable.

It is possible to rule out this mechanism by a careful analysis of the intensity data. The relative yield of HCl^+/VCl (i.e., HCl^+ produced from VCl) vs HCl^+/HCl (HCl^+ produced from room temperature HCl) at energies where both VCl and HCl display a quadratic intensity dependence is approximately 100, while at saturation it is 30 [see Figs. 2(b) and 2(c)]. These numbers do not take into account the quantum yield for HCl elimination from VCl. The relative yield of Cl vs HCl has been reported to lie between 0.5 and 1.4 (Table II). The absolute quantum yield for HCl at 180 nm has been reported as only 10%.[10] We will assume conservatively that the quantum yield of HCl at 193 nm is 50%. The fraction of HCl produced with $v=1$ is $<50\%$.[3,42] We conclude, therefore, that the relative yield R of HCl^+/VCl vs HCl^+/HCl is approximately 400 at low energies and approximately 120 at saturation. We also found that the saturation intensity for HCl^+/VCl is equal to or slightly less than that for HCl^+/HCl.

We will now show that these observations are inconsistent with the modified Rossi–Helm mechanism. First, we have estimated the magnitude of resonance enhancement of the two-photon ionization rate by the $A\ ^1\Pi$ state. The details of this calculation are presented in the Appendix. What we find is that vibrational excitation of HCl increases its ionization rate by no more than a factor of 10 (i.e., by the increased Franck–Condon overlap with the continuum wave function). This is one to two orders of magnitude smaller than required to explain our data.

We find that our saturation measurements are also inconsistent with the modified Rossi–Helm mechanism. Let $k_1(v)$, $k_2(v)$, and $k_d(v)$ denote, respectively, the rate constants for reactions (12a)–(12c) with $v=0$ or 1. The ratio of yields at low fluence is given by

$$R=[k_1(1)/k_1(0)][k_2(1)/k_2(0)]. \tag{17}$$

[see the discussion following Eq. (13)]. Taking $R=400$ and $k_1(1)/k_1(0)=10$, we deduce that $k_2(1)/k_2(0)=40$. According to Eq. (14) the yield ratio at saturation is

$$R_{sat}=[k_2(1)/k_2(0)]/[k_2'(1)/k_2'(0)], \tag{18}$$

where

$$k_2'(v)=k_2(v)+k_d(v). \tag{19}$$

For $R_{sat}=120$, $k_2(1)/k_2(0)=40$ implies that $k_2'(1)/k_2'(0)=0.33$. We expect, however, that this ratio should be greater than unity, since on a repulsive surface, the dissociation rate should increase with total energy. Also, since we observe that HCl^+/VCl saturates at slightly lower energy than HCl^+/HCl, we expect $k_2'(1)t$ in Eq. (14) to be slightly larger than $k_2'(0)t$.[43]

The Rossi–Helm mechanism is actually only one of three possible mechanisms for multiphoton ionization of VCl,

$$\begin{array}{lll} VCl^+ \xrightarrow{h\nu} HCl^+, & & \text{(model III)} \\ \uparrow h\nu & & \\ VCl^* \xrightarrow{h\nu} HCl^* + C_2H_2 \xrightarrow{h\nu} HCl^+, & & \text{(model II)} \\ \uparrow h\nu & & \\ VCl \xrightarrow{h\nu} HCl + C_2H_2 \xrightarrow{2h\nu} HCl^+. & & \text{(model I)} \end{array}$$

At issue is whether the second and third photons are absorbed by the parent molecule (the parent "ladder") or by a neutral fragment. In the Rossi–Helm mechanism (model I), the parent molecule dissociates into neutral fragments after absorbing only one photon. The HCl fragment is then ionized by two more photons. In an alternate mechanism (model III), the parent molecule is ionized by two photons and then is dissociated by a third photon to produce $C_2H_2 + HCl^+$. An intermediate case (model II) is one in which one photon produces electronically excited vinyl chloride, a second photon dissociates it into ground state C_2H_2 and electronically excited HCl* (a ladder switching step), and a third photon ionizes HCl*,

$$C_2H_3Cl + h\nu \rightarrow C_2H_3Cl^*, \tag{20}$$

$$C_2H_3Cl^* + h\nu \rightarrow C_2H_2 + HCl^*, \tag{21}$$

and

$$HCl^* + h\nu \rightarrow HCl^+ + e^-. \tag{22}$$

We can rule out model III since we do not observe any parent ions. In order for 90% of the parent ions to be dissociated by the third photon at a fluence of 3 mJ/cm^2, the absorption cross section of VCl^+ would have to be 8×10^{-16} cm^2. In comparison, the peak absorption cross section of ground state vinyl chloride (which has an oscillator strength of 0.4) is only 4×10^{-17} cm^2.[2]

An interesting question is the identity of the excited state of vinyl chloride produced in reaction (20). One possibility is the S_1 state invoked by Umemoto *et al.*[1] and shown in our Fig. 6. Another possibility is an (n,π^*) valence state which has not yet, to our knowledge, been reported spectroscopically. It is plausible that this long-lived state is also the one that produces the low energy Cl atoms. In a bulb experiment, Fahr and Laufer[10] obtained evidence for a reservoir state which lasts several microseconds and eventually decays to triplet vinylidene+HCl. They propose that their intermediate is a triplet (π,π^*) state. Additional experiments are required to characterize the spectroscopic properties of the long-lived state responsible for HCl^+ production that we have revealed in the present study.

VI. CONCLUSIONS

In this paper, we have reported angular distributions and Doppler profiles of chlorine and hydrogen atom photofragments from chloroethylenes (CH_2CHCl, *t*-$CHClCHCl$, CH_2CCl_2, CCl_2CClH) at 193 nm, as well as energy dependence measurements for the relative yields of H, Cl, HCl, and HCl^+ produced from vinyl chloride. For Cl fragments, our data, in conjunction with the translational energy distribution of Umemoto *et al.*,[1] show that the atom is detached by two mechanisms. The first is an isotropic pathway, resulting from the crossing of a repulsive (n,σ^*) state with a long-lived state. The translational energy distribution of this Cl fragment can be described by the Zamir–Levine formula. The second is an anisotropic pathway, resulting from direct dissociation on an (n,σ^*) surface. The translational energy distribution for this component can be described by a Gaussian function.

For the C–H detachment process, the angular distributions are isotropic and the translational energy distribution can be fit by a Maxwell–Boltzmann function. We propose a modified statistical model in which we assume that only atoms bonded to the same carbon atom participate actively in the energy distribution. This model can be used to explain the average translational energy for several other C–H photodissociation processes.

The HCl^+ fragment is produced by a three-photon resonant process. The initial step is the production of a long-lived state of vinyl chloride which can either dissociate to give ground state fragments or absorb another photon to give an electronically excited HCl fragment. We speculate that this long-lived state may be the same one that produces the isotropic Cl fragment.

APPENDIX: RESONANCE ENHANCEMENT OF THE TWO-PHOTON IONIZATION OF HCl

The two-photon ionization rate may be written as the square of the integral[44]

$$Q = I^2 \int \{\langle v|\mu|\omega\rangle\langle\omega|\mu|f\rangle/[\omega-\omega_L+i\Gamma]\}\rho(\omega)d\omega. \tag{23}$$

In Eq. (23), I is the laser intensity, μ is the dipole operator, $|v\rangle$ is the ground state with vibrational quantum number $v=0$ or 1, $|\omega\rangle$ is the intermediate continuum state with energy $\hbar\omega$ and decay rate Γ, $\rho(\omega)$ is the density of states of the continuum, $|f\rangle$ is the ionic state, and $\hbar\omega_L$ is the photon energy.

To evaluate this integral, we made several approximations. First, we assumed that $\langle\omega|\mu|f\rangle$ is not sensitive to v or ω and may be taken out of the integral. Second, we factored out the Franck–Condon factor from $\langle v|\mu|\omega\rangle$. The overlap integral $\langle v|\omega\rangle$ was evaluated analytically,[45] treating the ground state as a harmonic oscillator and using the potential energy function of Givertz and Balint-Kurti[39] for the $A\ ^1\Pi$ continuum state. Third, we treated Γ as a phenomenological parameter. We may estimate Γ as V/R, where V is the recoil velocity and R is a characteristic distance. For example, for $R=1$ Å, $\Gamma=1000$ cm^{-1} at 193 nm.

We evaluated Eq. (23) numerically for $v=0$ and 1 and $\Gamma=10$, 100, and 1000 cm^{-1}. In each case, we found that Q^2 increases by less than a factor of 10. That is, the main effect of vibrational excitation is to increase $\langle v|\omega\rangle$.

ACKNOWLEDGMENTS

M.K. acknowledges a grant-in-aid from the Ministry of Education, Science and Culture of Japan for partial support of this work. T.S. and K.T. thank the JSPS Fellowship for Japanese Junior Scientists. R.J.G. thanks the National Science Foundation (Grant No. CHE-9112591) and the Petroleum Research Fund, as administered by the American Chemical Society (Grant No. 21288-AC6), for its partial support. He also wishes to thank the Yamada Foundation for a travel grant to visit Hokkaido University where this manuscript was written.

[1] M. Umemoto, K. Seki, H. Shinohara, U. Nagashima, N. Nishi, M. Kinoshita, and R. Shimada, J. Chem. Phys. **83**, 1657 (1985).
[2] M. J. Berry, J. Chem. Phys. **61**, 3114 (1974), and references therein.
[3] D. J. Donaldson and S. R. Leone, Chem. Phys. Lett. **132**, 240 (1986).
[4] M. J. Rossi and H. Helm, J. Chem. Phys. **87**, 902 (1987).
[5] S. Kato and K. Morokuma, J. Chem. Phys. **74**, 6285 (1981).
[6] T. R. Fletcher and S. R. Leone, J. Chem. Phys. **88**, 4720 (1988).
[7] S. Satyapal, G. W. Johnston, and R. Bersohn, J. Chem. Phys. **93**, 6398 (1990).
[8] St. J. Dixon-Warren, M. S. Matyjaszczyk, J. C. Polanyi, H. Rielly, and J. G. Shapter, J. Phys. Chem. **95**, 1333 (1991).
[9] P. T. A. Reilly, Y. Xie, and J. R. Gordon, Chem. Phys. Lett. **178**, 511 (1991).
[10] A. Fahr and A. H. Laufer, J. Phys. Chem. **89**, 2906 (1985).
[11] T. Fujimoto, A. M. Rennert, and M. H. J. Winjen, Ber. Bunsenges. Phys. Chem. **74**, 282 (1970).
[12] P. Ausloos, R. E. Rebbert, and M. H. J. Winjen, J. Res. Natl. Bur. Stand., Sect. A **77**, 243 (1973).
[13] M. G. Moss, M. D. Ensminger, and J. D. McDonald, J. Chem. Phys. **74**, 6631 (1981).
[14] J. B. Pedley, R. D. Naylor, and S. P. Kirby, *Thermochemical Data of Organic Compounds*, 2nd ed. (Chapman and Hall, London, 1986).
[15] A. M. Wodtke and Y. T. Lee, in *Molecular Photodissociation Dynamics*, edited by M. N. R. Ashfold amd J. E. Baggott (Royal Society of Chemistry, London, 1987), pp. 31.
[16] K. M. Ervin, S. Gronert, S. E. Barlow, G. E. Giles, A. G. Harrison, V. M. Bierbaum, C. H. DePuy, W. C. Lineberger, and G. B. Ellison, J. Chem. Soc. **112**, 5750 (1990).
[17] Y. Osamura and H. F. Schaefer III, Chem. Phys. Lett. **79**, 412 (1981).
[18] The heats of formation at 298 K for the ground state molecules were taken from Ref. 14. The heat of formation of the ground state vinyl radical is the average of the values reported in Refs. 15 and 16. The energy of the first excited state of the vinyl radical was taken from Ref. 15. The heat of formation of ground state vinylidene is from Ref. 16, while the singlet–triplet spacing of vinylidene is taken from Ref. 17. The energy of reaction (2) is a rough estimate.
[19] Y. Matsumi, M. Kawasaki, T. Sato, T. Kinugawa, and T. Arikawa, Chem. Phys. Lett. **155**, 486 (1989).
[20] T. Arikawa, Jpn. J. Appl. Phys. **2**, 420 (1963).
[21] G. Iwata, Prog. Theor. Phys. **8**, 183 (1952); **9**, 97 (1953).
[22] Y. Xie, P. T. A. Reilly, S. Chilukuri, and R. J. Gordon, J. Chem. Phys. **95**, 854 (1991).
[23] E. C. Y. Inn, J. Atmos. Sci. **32**, 2375 (1975).
[24] J. A. Meyer and J. A. R. Samson, J. Chem. Phys. **52**, 266 (1970).
[25] R. Bersohn and S. H. Lin, Adv. Chem. Phys. **67**, 16 (1969).
[26] K. Tonokura, Y. Matsumi, M. Kawasaki, S. Tasaki, and R. Bersohn (to be published).
[27] (a) R. N. Zare and D. R. Herschbach, Proc. IEEE. **51**, 173 (1963); (b) R. Schmiedl, H. Dugan, and K. H. Welge, Z. Phys. A **304**, 137 (1982); (c) R. N. Dixon, J. Chem. Phys. **85**, 1866 (1986).
[28] E. Zamir and R. D. Levine, Chem. Phys. **52**, 253 (1980).
[29] P. M. Johnson, Acc. Chem. Res. **13**, 20 (1980).
[30] M. B. Robin, *Higher Excited States of Polyatomic Molecules* (Academic, New York, 1975), Vol. 2, p. 56.
[31] H. E. Hunziker, H. Kneppe, D. A. McLean, P. Siegbahn, and H. R. Wendt, Can. J. Chem. **61**, 993 (1983).
[32] *CRC Handbook of Chemistry and Physics*, edited by R. C. Weast and M. J. Astle (CRC, Boca Raton, FL, 1980).
[33] W. Yin, A. Chattopadhyay, and R. Bersohn, J. Chem. Phys. **94**, 5994 (1991).
[34] W. M. Jackson, D. S. Anex, R. E. Continetti, B. A. Balko, and Y. T. Lee, J. Chem. Phys. **95**, 7327 (1991).
[35] K. Tonokura, Y. Matsumi, M. Kawasaki, and K. Kasatani, J. Chem. Phys. **95**, 5065 (1991).
[36] A. E. Douglas and F. R. Greening, Can. J. Phys. **57**, 1650 (1979).
[37] W. Hill (private communication).
[38] J. A. Coxon, P. G. Hajigeorgiou, and K. P. Huber, J. Mol. Spectrosc. **131**, 288 (1988).
[39] S. C. Givertz and G. B. Balint-Kurti, J. Chem. Soc., Faraday Trans. 2 **82**, 1231 (1986).
[40] E. F. van Dishoeck, M. C. van Hemert, and D. Dalgarno, J. Chem. Phys. **77**, 3693 (1982).
[41] G. G. Balint-Kurti (private communication).
[42] According to Ref. 39, the absorption cross section for $v=2$ is 60 times smaller than for $v=0$, while that for $v=3$ and $v=4$ are approximately three and four times larger than for $v=0$. The populations for $v=1$ and $v>3$ are each approximately 20% (Refs. 2 and 3). Taking the effective fraction of vibrationally excited HCl as 50% is therefore a conservative estimate.
[43] We know that k_2 saturates before k_1. If the reverse were true, we would expect the HCl^+/VCl signal to saturate at ten times lower energy than HCl^+/HCl, since $k_1(1)=10k_1(0)$.
[44] S. H. Lin, Y. Fujimura, H. J. Neusser, and E. W. Schlag, *Multiphoton Spectroscopy of Molecules* (Academic, Orlando, 1984), p. 4.
[45] Y. B. Band and K. F. Freed, J. Chem. Phys. **63**, 338 (1975).